JAC

Disruption of D-alanyl esterification of *Staphylococcus aureus* cell wall teichoic acid by the β-lactam resistance modifier (−)-epicatechin gallate

Patricia Bernal, Mire Zloh and Peter W. Taylor*

School of Pharmacy, University of London, 29-39 Brunswick Square, London WC1N 1AX, UK

Objectives: The naturally occurring polyphenol (−)-epicatechin gallate (ECg) increases oxacillin susceptibility in *mecA*-containing strains of *Staphylococcus aureus*. Decreased susceptibility to lysostaphin suggests alterations to the wall teichoic acid (WTA) content of ECg-grown bacteria. Changes in WTA structure in response to ECg were determined.

Methods: Nuclear magnetic resonance spectroscopy of purified monomers from *S. aureus* was used to elucidate WTA structures. Molecular modelling of WTA chains was employed to determine their spatial configuration.

Results: ECg-grown methicillin-resistant *S. aureus* (MRSA) strains BB568 and EMRSA-16 displayed markedly reduced resistance to oxacillin, had thickened cell walls and separated poorly. Growth in ECg-supplemented medium reduced the substitution of the WTA backbone by D-alanine (D-Ala); ratios of *N*-acetyl glucosamine to D-Ala were reduced from 0.6 and 0.49 (for BB568 and EMRSA-16) to 0.3 and 0.28, respectively. Molecular simulations indicated a decrease in the positive charge of the bacterial wall, confirmed by increased binding of cationized ferritin, and an increase in WTA chain flexibility to a random coil conformation.

Conclusions: Structural elucidation and molecular modelling of WTA indicated that conformational changes associated with reduced D-Ala substitution may contribute to the increased susceptibility of MRSA to β-lactam antibiotics and account for other elements of the ECg-induced phenotype.

Keywords: epicatechin gallate, bacterial cell wall structure, β-lactam resistance, MRSA

Introduction

The steady rise in the incidence of infections due to *Staphylococcus aureus* resistant to second-generation β-lactam antibiotics such as methicillin and flucloxacillin [methicillin-resistant *S. aureus* (MRSA) strains] and their impact on treatment have been well documented.[1,2] Therapeutic options are further compromised by the tendency of staphylococci to accumulate genes conferring resistance to a range of non-β-lactam agents. Galloyl catechins, naturally occurring polyphenolic constituents of green tea,[3] have the capacity to reduce penicillin binding protein 2a (PBP2a)-mediated β-lactam resistance[4] and to disrupt the secretion of virulence-related proteins, such as coagulase and α-toxin,[5] by *S. aureus*. These abundant secondary metabolites

could offer a much-needed alternative approach to the treatment of intractable infections caused by MRSA and related pathogens. Following growth in medium containing either (−)-epigallocatechin gallate or (−)-epicatechin gallate (ECg), MRSA strains are sensitized to the bactericidal action of a wide range of β-lactam agents.[4] The non-galloyl equivalents (−)-epigallocatechin and (−)-epicatechin are unable to modulate the levels of β-lactam resistance, but have the capacity to potentiate galloyl catechin-mediated sensitization.[6] ECg, the most potent β-lactam modifier, and other catechins interact with lipid bilayers via hydrophobic domains[7–9] and their capacity to reduce β-lactam resistance correlates closely with their degree of penetration into the phospholipid palisade.[6] Galloyl catechins also promote cell wall thickening and cell aggregation,[10] reduce slime production and inhibit the

*Corresponding author. Tel/Fax: +44-20-753-5867; E-mail: peter.taylor@pharmacy.ac.uk

formation of staphylococcal biofilms.[11,12] ECg does not suppress transcription of *mecA* or production of its product, PBP2a; sensitization to β-lactam antibiotics is due to a more complex and incompletely defined mechanism.[12] The polyphenol elicits some changes in the levels of PBPs 1 and 3 in the staphylococcal membrane, resulting in a 5% to 10% reduction in peptidoglycan cross-linking; this modification is insufficient to compromise cell integrity.[12] In addition, ECg promotes retention of autolysins, enzymes that play a key role in cell separation and peptidoglycan turnover in the cell wall, probably in a predominantly inactive form.[12]

Lysostaphin is a peptidoglycan hydrolase that cleaves pentaglycine cross-bridges between glycan strands within peptidoglycan.[13] Growth of MRSA in broth supplemented with ECg markedly decreases susceptibility to lysostaphin.[12] Peptidoglycan−wall teichoic acid (WTA) complexes extracted from cells grown in ECg-supplemented medium are less susceptible to lysostaphin hydrolysis than complexes from bacteria grown in non-supplemented medium; after removal of WTA, rates of peptidoglycan hydrolysis by lysostaphin were essentially identical, regardless of the source of substrate.[12] These data suggest that ECg induces alterations in the composition, structure or conformation of WTA; these poly-D-ribitol-phosphate wall components[14] are known to affect methicillin susceptibility.[15] In order to shed light on the molecular basis of the β-lactam-susceptible phenotype, we have examined WTA from ECg-grown MRSA in relation to bacterial cell morphology and surface charge properties.

Materials and methods

Bacterial strains and reagents

S. aureus BB568 (a homogeneous methicillin-resistant strain that constitutively expresses PBP2a) was provided by B. Berger-Bächi, Institute of Medical Microbiology, University of Zürich. The epidemic MRSA isolate EMRSA-16 was isolated from a clinical sample at the Royal Free Hospital, London, UK. ECg was a gift from Y. Hara, Mitsui Norin, Tokyo, Japan. Oxacillin was purchased from Sigma-Aldrich. Bacteria were grown in Mueller−Hinton broth (MHB; Oxoid). MICs were determined as described previously.[4]

Purification of peptidoglycan−WTA complexes

ECg was dissolved in 50% v/v ethanol and added to batches (a series of 1−10 L batches were employed in order to accumulate sufficient material for analyses) of MHB to give a final concentration of 12.5 mg/L; the same volume (0.5 mL) of the vehicle was added to control flasks. Cultures were incubated at 37°C in an orbital incubator (180 rpm) and harvested by centrifugation once the OD_{660} had reached 0.6−0.7. Murein was prepared using a procedure adapted from Strandén *et al.*,[16] cells were suspended in 10 mL of 2 M NaCl and disrupted with 0.1 mm sterilized glass beads using a FastPrep® instrument (Qbiogene) for 45 s at speed setting 6. Cell wall fragments were recovered by centrifugation (14 100 **g**; 4 min), the pellet suspended in phosphate-buffered saline (PBS) and the glass beads allowed to settle to the bottom of the tube. Wall material was washed three times with 30 mL of 0.5% w/v sodium dodecyl sulphate and three times with water; it was then suspended in 30 mL of water and incubated with gentle stirring at 60°C for 30 min to remove non-covalently bound components. Cell walls were recovered by centrifugation, washed with 30 mL of water and covalently bound protein A removed by incubation at 37°C with 20 mL of

trypsin (0.2 mg/mL) in 0.15 mM Tris−HCl pH 7.0 for 18 h with stirring. After recovery by centrifugation, wall material was washed with 1 M Tris−HCl, 1 M Tris−HCl containing 1 M NaCl, again with 1 M Tris−HCl (all pH 7.0) and three times with water.

Hydrolysis of peptidoglycan−WTA complexes

Teichoic acid was released from peptidoglycan−WTA using 10% w/v aqueous trichloroacetic acid (TCA) at 4°C for 18 h. Peptidoglycan was removed by centrifugation (5526 **g**; 45 min; room temperature) and WTA precipitated from the supernatant with 0.1 vol of 3 M sodium acetate pH 5.1 in 3 vol of 95% ice-cold ethanol and held overnight at −80°C. After centrifugation (5526 **g**; 30 min; room temperature), the pellet was washed five times with 95% ethanol; after the final ethanol wash, the solvent was allowed to evaporate, purified WTA was lyophilized and stored at −20°C. The hydrolysis procedure released WTA in its D-alanine (D-Ala)-substituted monomeric form.

Hydrolysis of peptidoglycan by lysostaphin

Purified peptidoglycan−WTA was suspended to OD_{600} 0.5 in 50 mM Tris−HCl pH 7.5 containing 145 mM NaCl and 4 U lysostaphin (Sigma-Aldrich). The rate of hydrolysis was determined by measuring reduction in OD_{600} during incubation at 37°C. For the determination of the rate of hydrolysis of peptidoglycan, WTA was removed from samples with 10% v/v TCA at 4°C for 24 h and WTA-free peptidoglycan was recovered by centrifugation, followed by washing with water.

Electron microscopy

For scanning electron microscopy (SEM), bacteria were recovered by centrifugation and washed twice with PBS. Cells were fixed in 1.5% w/v glutaraldehyde for at least 2 h at room temperature, washed once with 70% ethanol and twice with 100% ethanol. Air-dried, gold-coated preparations were examined using an FEI XL30 scanning electron microscope. For transmission electron microscopy (TEM), recovered, PBS-washed cells were fixed in glutaraldehyde as before, treated with osmium tetroxide and embedded in epoxy resin. Sectioning and staining with uranyl acetate were followed by Reynolds' lead citrate. Ultra-thin sections were viewed and photographed using a Philips 201 transmission electron microscope. Binding of cationized ferritin to the bacterial surface was determined according to Graham and Beveridge[17] using a final ferritin concentration of 16.6 mg/L.

NMR spectroscopy

Samples (20 mg) were dissolved in 10% D_2O−90% H_2O. Spectra were acquired at 298 K on a Bruker Avance NMR 500 MHz instrument (Bruker BioSpin) equipped with gradients and broadband probe. For structural elucidation, a set of 1D and 2D ^1H, ^{31}P and ^{13}C experiments with solvent pre-saturation were undertaken. Spectra were processed using Topspin 1.3 software (Bruker BioSpin).

Molecular modelling

Modelling was undertaken using Maestro graphics interface (Schrödinger LLC) and MacroModel 9.11;[18] poses were energy-minimized using the Merck molecular force field[19] and the influence of solvation free energy considered by the generalized Born/surface area continuum model.[20] Cut-off distances for non-bonded

interactions were as follows: 8 Å for van der Waals, 20 Å for electrostatic interactions and 4 Å for hydrogen bonding. Conformational searches employed Monte Carlo torsional sampling (5000 steps) on octomers; stochastic dynamic simulations on dodecamers were carried out using an established protocol.[21] Models obtained by conformational searches and stochastic simulations were complementary.

Results and discussion

ECg (12.5 mg/L) reduced the MIC of oxacillin for *S. aureus* BB568 and EMRSA-16 from 256 and 512 mg/L, respectively, to 1 mg/L. Growth in the presence of ECg induced morphological changes to strains EMRSA-16 and BB568. SEM of control cells (Figure 1a) indicated typically round or ovoid, loosely clumped cocci with smooth surfaces. In cells exposed to 12.5 mg/L ECg (Figure 1b), larger, poorly separated bacteria with a rougher surface were observed. Measurement using TEM of glutaraldehyde-fixed cells, sectioned mid-line through the longitudinal axis, determined the mean diameter of control cells to be 623 ± 10 nm (SEM; $n = 10$) and diameters of the more heterogeneous ECg-grown cell population to range from 550 to 950 nm. TEM of sections indicated that growth in ECg increased the thickness of the cell wall (Figure 1d) compared with control bacteria (Figure 1c) and the cells tended to remain as 'packets' rather than separate cleanly. The outer layer of the wall of ECg-grown cells was noticeably more fibrous in nature (Figure 1d) than that of controls (Figure 1c).

Growth in MHB supplemented with 12.5 mg/L ECg markedly decreased the susceptibility of MRSA strains BB568 and EMRSA-16 to lysostaphin; for both strains, the lysostaphin MIC was increased from 0.06 to >8 mg/L. Peptidoglycan–WTA complexes extracted from BB568 cells grown in MHB supplemented with 12.5 mg/L ECg were less susceptible to lysostaphin hydrolysis (24% hydrolysis in 50 min) than complexes from bacteria grown in non-supplemented medium (50% in 50 min); following removal of WTA, both the rate and the extent of peptidoglycan hydrolysis were indistinguishable regardless of ECg supplementation of the growth medium.

Cultures of BB568 or EMRSA-16 yielded 0.2–3.0 mg of WTA monomer per litre of broth culture, depending on the strain and the presence or absence of ECg in the growth medium. To obtain sufficient material for analysis by NMR, material obtained from several 1–10 L batches of culture was pooled prior to analysis. With NMR, structural assignment was achieved by manual examination of ^{1}H–^{1}H, ^{1}H–^{31}P and ^{1}H–^{13}C correlations in 2D homonuclear (correlation spectroscopy) and 2D heteronuclear (heteronuclear single quantum coherence, heteronuclear multiple quantum coherence and heteronuclear multiple bond coherence) spectra. Full assignments of all spectra were achieved, and the chemical shifts obtained (Table 1) for the D-ribitol-5-phosphate and *N*-acetyl glucosamine (GlcNAc) constituents were in good agreement with the known assignments for monomers derived from the $(1\rightarrow5)$-linked poly(ribitol phosphate) WTA elaborated by *S. aureus* MN8m.[22] The methyl group of D-Ala ($\delta = 1.538$) was clearly differentiated from the methyl group of GlcNAc (Figure 3b; $\delta = 2.006$), enabling quantification of the extent of D-Ala esterification of the monomeric units (Figure 2a). D-Ala substitution also influenced the resonant frequency of the ^{31}P signal: $\delta = 0.4$ ppm for D-Ala-esterified WTA and $\delta = 1.1$ ppm for non-esterified monomer. The fully assigned spectra are presented as Supplementary data [see Figure S1 available at *JAC* Online (http://jac.oxfordjournals.org/)].

The molar ratios of constituent WTA monomer units were determined by the comparison of the area under the peak of corresponding groups (Figure 2b). Thus, the ribitol phosphate
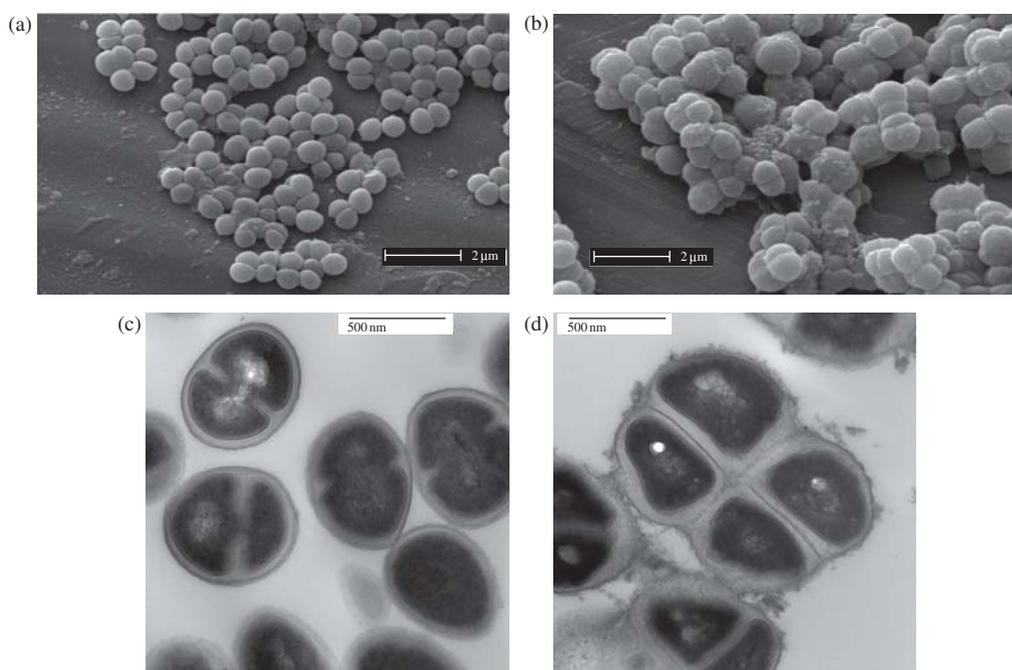

Figure 1. SEM (a and b) and TEM (c and d) images of *S. aureus* EMRSA-16 grown to mid-logarithmic phase in the absence (a and c) and presence (b and d) of 12.5 mg/L ECg. Essentially identical images were obtained using BB568.

Table 1. [1]H, ^{13}C and ^{31}P chemical shifts (δ ppm) of WTA from *S. aureus* BB568 and EMRSA-16[a]

Unit/NMR type	Chemical shift (δ ppm)					
	1/1′	2	3/3′	4	5/5′	6/6′
Rib[b]						
[1]H	3.9/4.05	3.83	3.84	4.068	3.87/4.071	
[13]C	66.77	70.3	71.09	79.38	64.95	
[31]P	1.1					
β-GlcNAc						
[1]H	4.65	3.68	3.486	3.381	3.38	3.66/3.83
[13]C	101.38	55.78	74.78	70.00	75.78	60.73
Rib+D-Ala						
[1]H	3.9/4.05	5.33	4.05	4.068	4.071	
[13]C	66.7	74.78	66.77	79.38	64.95	
[31]P	0.4					
Ala						
[1]H		4.18	1.538			
[13]C	170.0	49.11	15.51			
NAc						
[1]H		2.006				
[13]C	175.08	22.472				

[a]The 1D ^{1}H spectrum with water was acquired using a sweep width of 10330 Hz and 65536 data points, giving 256 transients. The 1D ^{13}C spectra were acquired using a sweep width of 30030 Hz and 131072 data points, giving 26000 transients. The 2D HMQC (pulse program inv4gpqf) and HMBC (pulse program inv4gplplrndqf) spectra were acquired with 1024 data points in direct dimensions (sweep width 4882 Hz) and 256 complex points (sweep width 31440).
[b]Rib, ribitol; GlcNAc, *N*-acetyl glucosamine; D-Ala, D-alanine; NAc, *N*-acetyl.

backbone units are universally glycosylated at position 4 but variably substituted at C2 with D-Ala (Figure 2a). The ratios of GlcNAc to D-Ala in WTA extracted from BB568 and EMRSA-16 grown in the absence of ECg were 0.6 and 0.49, respectively, as indicated by ^{1}H NMR (Table 2). When ECg (12.5 mg/L) was incorporated into the MHB growth medium, the degree of D-alanylation was significantly reduced to 0.3 for BB568 and 0.28 for EMRSA-16. The decreases in D-Ala content in response to exposure to ECg were confirmed by ^{31}P NMR (Table 2).

Changes in the degree of D-alanylation can have profound effects on the conformation and charge characteristics of the staphylococcal surface. The D-alanyl ester content of WTA is highly variable and subject to modulation by environmental influences such as pH, temperature and NaCl and Mg^{2+} concentrations.[14] The amino group of D-Ala, with a predicted pK_a of 8.42, is protonated at neutral pH, conferring a positive charge on the D-Ala moiety. In this protonated state, the amino group has the capacity to form ion pairs with phosphodiester either up or down the chain,[14] inducing two distinct energy-minimized conformational states. To examine the effect of different degrees of D-Ala substitution on predicted WTA conformation, we carried out *in silico* conformational searches and stochastic simulations on octameric and dodecameric (1→5)-linked poly-D-ribitol-phosphate-GlcNAc chains. The position of D-Ala residues along the chain was randomized to reflect the even distribution of esters in purified polymers.[14] As anticipated, the charge distribution on the chain surface was heavily influenced by D-Ala content (Figure 3a). Chains with a GlcNAc-to-D-Ala ratio of 0.6, simulating WTA extracted from BB568 grown in the absence of

ECg, displayed a mainly positively charged surface; these charges corresponded to the amino groups of D-Ala. Negative surfaces are more prominent on WTA from EMRSA-16 control cells (0.49), whilst mainly negative surfaces can be observed in chains with a ratio (0.3) simulating ECg-induced WTA. Consistent with these predictions is the observation that ECg-treated cells bound more cationized ferritin than controls when examined by TEM (Figure 4). Modelling also indicated that D-Ala might affect chain flexibility. The hydrogen bonds that form between amine and phosphate groups[14] decrease the potential for free rotation within each unit, decreasing flexibility. Our simulations (Figure 3b) indicate that such hydrogen bonding results in the formation of an extended chain when the GlcNAc:D-Ala ratio is 0.49, and an ECg-induced reduction to 0.3 results in increased chain flexibility, producing a random coil conformation reminiscent of that proposed for WTA at high ionic strength.[23] Interestingly, modelling of WTA with a ratio of 0.6, corresponding to the polymer from BB568 control cells, suggests that when the degree of D-Ala substitution is relatively high, chains are inflexible but are not extended compared with 0.49 octomers, due to the constraints imposed by hydrogen bonding between D-Ala residues and non-neighbouring phosphate groups, causing kinks in chain conformation (Figure 3b). These changes in the conformation of WTA may explain differences in the packing of EMRSA-16, BB568 and ECg-treated cells: equivalent amounts of bacteria (mg of dry weight) recovered from MHB occupy volumes corresponding to the hydrodynamic volume of the cell wall predicted by our simulations (data not shown).
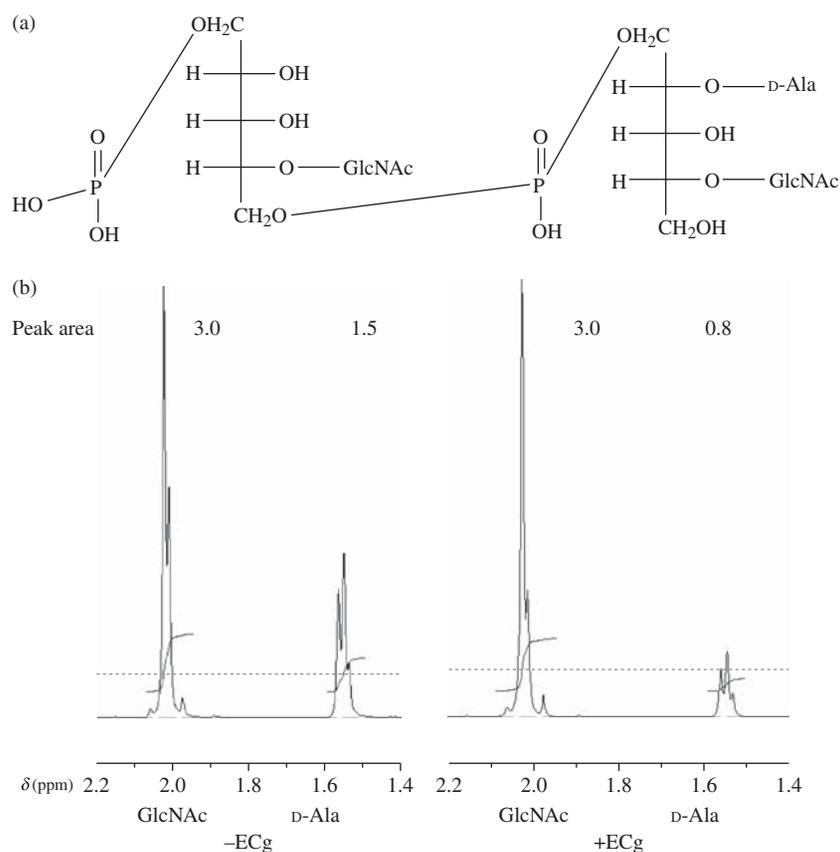
Figure 2. Schematic structure of WTA: two units of the variable length (1→5)-linked poly-D-ribitol-phosphate-GlcNAc chain are shown, one substituted with D-Ala at C2 of the ribitol moiety (a). ^{1}H-NMR spectra show GlcNAc and D-Ala peaks of WTA extracted from non-treated cells and cells exposed to 12.5 mg/L ECg (b).

It is tempting to speculate that the conformational changes induced by ECg are responsible for the observed decreases in the susceptibility of peptidoglycan–WTA complexes to lysostaphin, with the random movement of the WTA chains restricting access of the enzyme to the pentaglycine cross-bridges. Changes in chain conformation may also lead to different packing arrangements for WTA within the cell wall, with our data indicating that packing efficiency may be highest at a ratio of 0.49 and lowest at 0.3, and that this may also impact on enzymatic hydrolysis. The main conclusion drawn from this study, that growth in the presence of ECg produces large reductions in D-alanylation of WTA, provides a rationale for some aspects of the complex galloyl catechin-induced phenotype. For example, *dlt* mutants of *S. aureus*, lacking the capacity to synthesize or attach D-Ala esters to teichoic acids, lose their ability to form biofilms on polystyrene or glass surfaces due to electrostatic repulsion resulting from a stronger negative surface charge.[24] Similarly, a reduction in D-alanylation is likely to account for our observation[12] that ECg elicits retention of autolysins within the cell wall. There is good evidence[14] that the number of binding sites for autolysins within the cell wall is in part determined by the degree of D-alanylation of teichoic acids: these enzymes require anionic sites for their retention, although the role played by wall matrix charge characteristics in the modulation of autolytic activity is less clear.

Reductions in D-alanylation are correlated with increases in susceptibility to cationic antibacterial peptides[25] and

Table 2. Ratio of D-Ala:GlcNAc in WTA from *S. aureus* BB568 and EMRSA-16 grown in the presence and absence of 12.5 mg/L ECg

Strain and treatment	NMR type	
	^{1}H	^{31}P
BB568	0.6[a]	
BB568+ECg	0.3	
EMRSA-16	0.49 (0.42–0.56)	0.6
EMRSA-16+ECg	0.28 (0.26–0.30)	0.23

[a]For ^{1}H NMR spectra, D-Ala:GlcNAc ratios represent the mean of three determinations (range).

glycopeptide antibiotics such as vancomycin,[26] but the role of D-Ala in modulating resistance to β-lactam agents, which are anionic at physiological pH, is less well understood. *dlt* mutants of *Bacillus subtilis* are more susceptible to methicillin than the parent strain.[15] However, Nakao *et al.*[27] reported that insertional mutagenesis of genes in the *dlt* operon of an *S. aureus* clinical isolate with a relatively low level of methicillin resistance (16 mg/L) resulted in a decrease in methicillin susceptibility, although the authors did not demonstrate a reduction in D-alanylation of teichoic acids. Our data tend to favour a role for
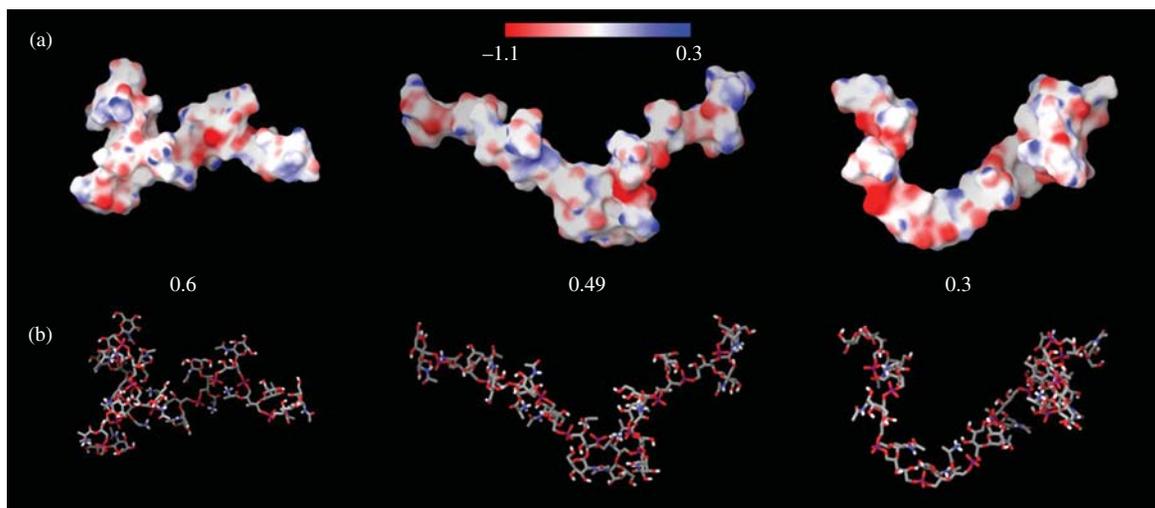
Figure 3. Molecular electrostatic potential surfaces (a) and stick representation (b) of WTA substituted with D-Ala (ratios GlcNAc:D-Ala are 0.6, 0.49 and 0.3). Three-dimensional models were obtained by conformational search and consisted of 5000 steps of Monte Carlo torsional sampling after initial model building and minimization. The scale at the top of the figure indicates colour-coded values of the electrostatic potential mapped onto the molecular surface: blue indicates positive and red negative potential, within the range −1.1 to 0.3.
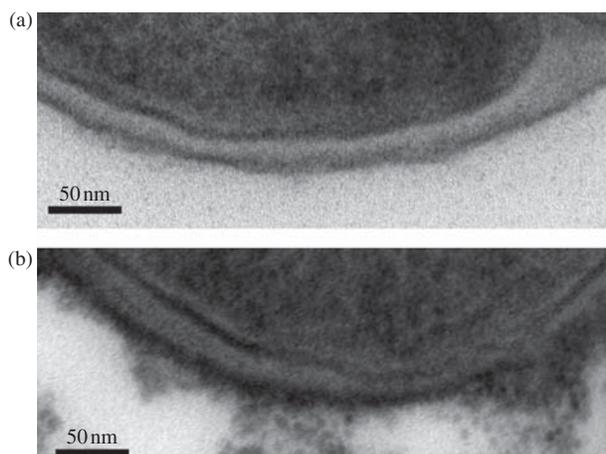

Figure 4. TEM images of *S. aureus* EMRSA-16 incubated with cationized ferritin after growth in the absence (a) or presence (b) of 12.5 mg/L ECg.

D-Ala in the modulation of β-lactam resistance, although it is likely that the very large reductions in MIC that we observe can only be explained by interruption of *mecA*-mediated resistance, and it is at present unclear how D-alanylation of WTA can impact on such a process. Thus, our current work could indicate that PBP2a is only functional in the presence of teichoic acids that are properly D-alanylated. However, the ionic charge imparted by teichoic acids influences the stability and folding of proteins in the cell wall through modulation of divalent cation binding to teichoic acids.[14] Further, teichoic acids may affect the phase transition profile of phospholipid bilayers, at least in model systems.[28] These events may impact on the function of membrane and wall enzymes, such as PBP2a, involved in β-lactam resistance and may compromise the capacity of PBPs to target the septum during cell division, determining the ECg-induced phenotype. We are currently investigating the biophysical properties of the cytoplasmic membrane from ECg-treated staphylococci in an attempt to determine the relevance of such observations to the modulation of β-lactam resistance.

Acknowledgements

Funding

Transparency declarations

None to declare.

Supplementary data

Figure S1 is available as Supplementary data at *JAC* Online (http://jac.oxfordjournals.org/).

References

1. Diep BA, Chambers HF, Graber CJ *et al.* Emergence of multidrug-resistant, community-associated, methicillin-resistant *Staphylococcus aureus* clone USA300 in men who have sex with men. *Ann Intern Med* 2008; **148**: 249–57.

2. Francois P, Harbarth S, Huyghe A *et al.* Methicillin-resistant *Staphylococcus aureus*, Geneva, Switzerland, 1993–2005. *Emerg Infect Dis* 2008; **14**: 304–7.

3. Taylor PW, Hamilton-Miller JMT, Stapleton PD. Antimicrobial properties of green tea catechins. *Food Sci Technol Bull* 2005; **2**: 71−81.

4. Stapleton PD, Shah S, Anderson JC *et al*. Modulation of β-lactam resistance in *Staphylococcus aureus* by catechins and gallates. *Int J Antimicrob Agents* 2004; **23**: 462−7.

5. Shah S, Stapleton PD, Taylor PW. The polyphenol (−)-epicatechin gallate disrupts the secretion of virulence-related proteins by *Staphylococcus aureus*. *Lett Appl Microbiol* 2008; **46**: 181−5.

6. Stapleton PD, Shah S, Hara Y *et al*. Potentiation of catechin gallate-mediated sensitization of *Staphylococcus aureus* to oxacillin by non-galloylated catechins. *Antimicrob Agents Chemother* 2006; **50**: 752−5.

7. Kajiya K, Kumazawa S, Nakayama T. Steric effects on the interaction of tea catechins with lipid bilayers. *Biosci Biotechnol Biochem* 2001; **65**: 2638−43.

8. Kajiya K, Kumazawa S, Nakayama T. Effects of external factors on the interaction of tea catechins with lipid bilayers. *Biosci Biotechnol Biochem* 2002; **66**: 2330−5.

9. Caturla N, Vera-Samper E, Villalain J *et al*. The relationship between the antioxidant and antibacterial properties of galloylated catechins and the structure of phospholipid model membranes. *Free Radic Biol Med* 2003; **34**: 648−62.

10. Hamilton-Miller JMT, Shah S. Disorganization of cell division of methicillin-resistant *Staphylococcus aureus* by a component of tea (*Camellia sinensis*): a study by electron microscopy. *FEMS Microbiol Lett* 1999; **176**: 463−9.

11. Blanco AR, Sudano-Roccaro A, Spoto GC *et al*. Epigallocatechin gallate inhibits biofilm formation by ocular staphylococcal isolates. *Antimicrob Agents Chemother* 2005; **49**: 4339−43.

12. Stapleton PD, Shah S, Ehlert K *et al*. The β-lactam-resistance modifier (−)-epicatechin gallate alters the architecture of the cell wall of *Staphylococcus aureus*. *Microbiology* 2007; **153**: 2093−103.

13. Iversen OJ, Grov A. Studies on lysostaphin. Separation and characterization of three enzymes. *Eur J Biochem* 1973; **38**: 293−300.

14. Neuhaus FC, Baddiley J. A continuum of anionic charge: structures and functions of D-alanyl-teichoic acids in Gram-positive bacteria. *Microbiol Mol Biol Rev* 2003; **67**: 686−723.

15. Wecke J, Madela K, Fischer W. The absence of D-alanine from lipoteichoic acid and wall teichoic acid alters surface charge, enhances autolysis and increases susceptibility to methicillin in *Bacillus subtilis*. *Microbiology* 1997; **143**: 2953−60.

16. Strandén AM, Ehlert K, Labischinski H *et al*. Cell wall monoglycine cross-bridges and methicillin hypersusceptibility in a *femAB* null mutant of methicillin-resistant *Staphylococcus aureus*. *J Bacteriol* 1997; **179**: 9−16.

17. Graham LL, Beveridge TJ. Structural differentiation of the *Bacillus subtilis* 168 cell wall. *J Bacteriol* 1994; **176**: 1413−21.

18. Mohamadi F, Richards N, Guita W *et al*. MacroModel—an integrated software system for modeling organic and bioorganic molecules using molecular mechanics. *J Comput Chem* 1990; **11**: 440−67.

19. Cramer CJ, Truhlar DG. Continuum solvation models: classical and quantum mechanical implementations. *Rev Comput Chem* 1995; **6**: 1−72.

20. Still WC, Tempczyk A, Hawley RC *et al*. Semianalytical treatment of solvation for molecular mechanics and dynamics. *J Am Chem Soc* 1990; **112**: 6127−9.

21. Zloh M, Shaunak SW, Balan S *et al*. Identification and insertion of 3 carbon bridge in protein disulfide bonds: a computational approach. *Nat Prot* 2007; **2**: 1070−83.

22. Vinogradov E, Sadovskaya I, Li J *et al*. Structural elucidation of the extracellular and cell wall teichoic acids of *Staphylococcus aureus* MN8m, a biofilm forming strain. *Carbohydr Res* 2006; **341**: 738−43.

23. Pal MK, Ghosh TC, Ghosh JK. Studies on the conformation of and metal ion binding by teichoic acid of *Staphylococcus aureus*. *Biopolymers* 1990; **30**: 273−7.

24. Gross M, Cramton SE, Götz F *et al*. Key role of teichoic acid net charge in *Staphylococcus aureus* colonization of artificial surfaces. *Infect Immun* 2001; **69**: 3423−6.

25. Peschel A, Otto M, Jack RW *et al*. Inactivation of the *dlt* operon in *Staphylococcus aureus* confers sensitivity to defensins, protegrins, and other antimicrobial peptides. *J Biol Chem* 1999; **274**: 8405−10.

26. Peschel A, Vuong C, Otto M *et al*. The D-alanine residues of *Staphylococcus aureus* teichoic acids alter the susceptibility to vancomycin and the activity of autolytic enzymes. *Antimicrob Agents Chemother* 2000; **44**: 2845−7.

27. Nakao A, Imai S, Takano T. Transposon-mediated insertional mutagenesis of the D-alanyl-lipoteichoic acid (*dlt*) operon raises methicillin resistance in *Staphylococcus aureus*. *Res Microbiol* 2000; **151**: 823−9.

28. Riske KA, Döbereiner H-G, Lamy-Freund MT. Gel−fluid transition in dilute versus concentrated DMPG aqueous dispersions. *J Phys Chem Ser B* 2002; **106**: 239−46.